Leveraging propionate-induced growth inhibition in *Corynebacterium glutamicum* to evolve improved methylmalonyl-CoA-dependent polyketide production

Jay Keasling (jdkeasling@lbl.gov)
Joint BioEnergy Institute https://orcid.org/0000-0003-4170-6088
chunjun zhan
Joint BioEnergy Institute
Namil Lee
Joint BioEnergy Institute
Guangxu Lan
Lawrence Berkeley National Laboratory https://orcid.org/0000-0002-0415-5849
Qingyun Dan
Joint BioEnergy Institute
Aidan Cowan
Joint BioEnergy Institute
Zilong Wang
Joint BioEnergy Institute
Edward Baidoo
Joint BioEnergy Institute
Ramu Kakumanu
Joint BioEnergy Institute
Bridget Luckie
Joint BioEnergy Institute
Rita Kuo
Joint BioEnergy Institute
Joshua McCauley
Joint BioEnergy Institute
Robert Haushalter
Joint BioEnergy Institute

Article

Keywords: Corynebacterium glutamicum, Polyketide synthase, Propionate, Germicidin synthase, Citrate synthase

Posted Date: October 28th, 2022

DOI: https://doi.org/10.21203/rs.3.rs-2200679/v1

Version of Record: A version of this preprint was published at Nature Metabolism on July 13th, 2023. See the published version at https://doi.org/10.1038/s42255-023-00830-x.

Abstract

Corynebacterium glutamicum is a promising host for production of valuable polyketides. Propionate addition, a strategy known to increase polyketide production by increasing intracellular methylmalonyl-CoA availability, causes growth inhibition in *C. glutamicum*. The mechanism of this inhibition was unclear prior to our work. Here we provide evidence that accumulation of propionyl- and methylmalonyl-CoA induces growth inhibition in *C. glutamicum*. We then show that growth inhibition can be relieved by introducing methylmalonyl-CoA-dependent polyketide synthases. With germicidin as an example, we used adaptive laboratory evolution (ALE) to leverage the fitness advantage of polyketide production in the presence of propionate to evolve improved germicidin production. Whole genome sequencing revealed mutations in germicidin synthase (Gcs), which improved germicidin titer, as well as mutations in citrate synthase, which effectively evolved the native glyoxylate pathway to a new methylcitrate pathway. Together, our results show that *C. glutamicum* is a capable host for polyketide production, and we can take advantage of propionate growth inhibition to drive titers higher by evolution.

Introduction

Polyketides are a remarkable class of natural secondary metabolites produced by bacteria[1], fungi[2, 3] and plants[4]. These natural products have drawn interest for decades owing to their valuable medicinal activities as antibacterial[5, 6], antifungal[7], antiparasitic[8], anticancer[9], and immunosuppressive[10] therapies. Polyketide biosynthesis initiates with a variety of starter molecules, which are subsequently extended using malonyl-CoA, methylmalonyl-CoA, or other malonyl-CoA derivatives. Recent sequence analyses revealed that 55% of acyltransferases (AT) in known PKSs are malonyl-CoA specific and 30% are methylmalonyl-CoA specific[11], which indicates that malonyl-CoA and methylmalonyl-CoA are the key precursors for polyketide production. Malonyl-CoA serves as the basic precursor for the biosynthesis of many cellular building blocks (e.g., fatty acids) and a variety of secondary metabolites. Many strategies, including supplementation with acetate[12, 13] and deleting competitive pathways[14], have been adopted to increase malonyl-CoA concentration[15].

In contrast, methylmalonyl-CoA, another crucial precursor for many polyketides, is not universally present in bacterial hosts[16]. Early work on expressing PKSs in heterologous hosts (e.g., *Escherichia coli*) explored several pathways to produce methylmalonyl-CoA[17]: addition of propionate and carboxylation of propionyl-CoA to methylmalonyl-CoA by propionyl-CoA carboxylase (PCCase), addition of succinate and isomerization to methylmalonyl-CoA by a heterologous mutase and epimerase[18], and addition of methylmalonate and activation by a heterologous CoA ligase MatB. In *E. coli*, it was found that propionate feeding resulted in the highest titers of polyketide products[19-21]. Analysis of carbon flux in these pathways demonstrated that compared with other common carbon sources like glucose, the propionate carboxylation pathway also results in less carbon loss to CO_2 (Extended Data Fig. S1), which is advantageous for production of commodity chemicals. As such, propionate may be a promising carbon source for methylmalonyl-CoA production.

Polyketide production has primarily utilized *streptomycetes* as hosts[22-24], which have the native propionate utilization pathway[19]. However, the slow growth rate, complex life cycles, and relative lack of high efficiency genetic engineering tools[25, 26] are major challenges for industrial scale-up of *Streptomyces* for production of many chemicals. *C. glutamicum,* an organism used to produce millions of tons of amino acids each year[27], has many features that make it a promising host for polyketide production. This industrial microbe can natively produce methylmalonyl-CoA through one of its native propionate utilization pathways[28, 29] (Fig. 1), has many genetic tools available[30, 31], and harbors native PKSs for production of specialized lipids[32]. Additionally, it is closely related to *Mycobacteria* and *Streptomyces*[33], which are rich sources of polyketide biosynthetic gene clusters. All of these factors indicate that it might be a good host for heterologous PKSs. Unfortunately, addition of propionate to CGXII minimal medium inhibits the growth of *C. glutamicum,* but the metabolic basis of this inhibition was unclear prior to our work.

C. glutamicum encodes two distinct pathways for catabolizing propionate. In the 2-methylcitrate pathway, propionate is oxidized to pyruvate while oxaloacetate is reduced to succinate via the intermediate 2-methylcitrate. This pathway is essential for growth on propionate as the sole carbon source in minimal media[28]. In the methylmalonyl-CoA pathway, an endogenous carboxylase converts propionyl-CoA to (S)-methylmalonyl-CoA, which is then epimerized to (R)-methylmalonyl-CoA by the enzyme encoded by *cgl1217* and isomerized to succinyl-CoA by the vitamin B12-dependent mutase (McmAB) (Fig. 1). Previous reports have suggested that accumulation of 2-methylcitrate is the cause of inhibition[34], but we show here that propionate addition still inhibits growth when the methylcitrate pathway is removed. It has been shown that addition of vitamin B12, the required cofactor for McmAB, relieves growth inhibition in the presence of propionate[35].

These previous results led us to hypothesize that accumulation of propionyl-CoA and methylmalonyl-CoA is responsible for growth inhibition, and pathways that convert methylmalonyl-CoA to free CoA-SH or another primary metabolite will impart a growth advantage to *C. glutamicum* in propionate-containing media. Here, we show that accumulation of propionyl- and methylmalonyl-CoA is the cause of growth inhibition by propionate in *C. glutamicum*, and blocking conversion of these CoAs to primary metabolites inhibits growth on propionate. Because conversion of methylmalonyl-CoA into succinyl-CoA was shown to relieve the propionate-induced growth lag, several methylmalonyl-CoA-consuming polyketide production pathways (germicidin synthase (Gcs) and an engineered lipomycin synthase) were introduced to provide a means of reducing the accumulation of intracellular methylmalonyl-CoA and producing free CoA-SH, relieving the growth inhibition. We found that polyketide production is correlated with a shorter lag phase when the cells expressing the PKS are grown in minimal media containing propionate. Furthermore, we demonstrated that addition of propionate can be used as a selective pressure for Adaptive Laboratory Evolution (ALE) of PKSs in *C. glutamicum*. Using ALE in the presence of propionate, we increased the titer of germicidin over 18-fold and thoroughly eliminated growth inhibition in propionate-containing medium. Next generation sequencing (NGS) and reverse engineering demonstrated that the evolved Gcs can improve germicidin production, and the

evolved citrate synthase (GltA2)-based methylcitrate pathway rescued cell growth by consuming propionyl-CoA and methylmalonyl-CoA. Taken together, our results show that *C. glutamicum* is not only capable of expressing PKSs, but also can be used as a platform to improve polyketide titers through directed evolution.

Results

1. Propionate induces growth inhibition when activated to propionyl-CoA

To determine whether inhibition is caused by free propionate or its metabolic derivatives, we first evaluated the propionate uptake and activation pathway (Fig. 2a). *C. glutamicum* can activate propionate using the acetate uptake pathway, including acetate kinase (Ack) and phosphotransacetylase (Pta)[28]. We deleted those two genes to generate strain Cz01. Compared with wild-type, the growth rate of Cz01 increased by 7% (Fig. 2b), and propionate consumption and the lag phase decreased by 60% and 40%, respectively (Fig. 2c and Extended Data Fig. 2). These results indicate that propionate must be activated to propionyl-CoA to induce growth inhibition. Besides the acetate uptake pathway, the CoA transferase (succinyl-CoA: acetate CoA-transferase) encoded by *cgl2569* may be another propionate activation pathway[36], catalyzing conversion of propionate to propionyl-CoA while succinate/acetate is produced by succinyl-CoA/acetyl-CoA consumption (Fig. 2a). To validate whether this pathway contributes to propionate-induced growth inhibition, we deleted *cgl2569* from the wild-type strain to generate strain Cz02 and evaluated its growth in propionate-containing medium. Cz02 grew faster (increased by 25%), consumed less propionate (decreased by 99%) and had a shorter lag phase (decreased by 50%), compared to the wild-type strain (Fig. 2b, c, and Extended Data Fig. S2). Additionally, we performed *in vitro* experiments using purified Cgl2569 protein, which showed that Cgl2569 can convert propionate to propionyl-CoA using either succinyl-CoA or acetyl-CoA as a CoA donor (Extended Data Fig. S3). Cgl2569 was overexpressed in wild-type and Cz02 to generate Cz19 and Cz22, respectively. Cell growth was further inhibited when *cgl2569* was overexpressed (Fig. 2d), consistent with the reasoning that the inhibition mechanism involves propionyl-CoA. Deletion of *cgl2569* particularly decreased the uptake of propionate (decreased by 99%) compared to deletion of the acetate uptake pathway (decreased by 60%) (Fig. 2b, c), which indicates that the *cgl2569* pathway is more active than the acetate uptake pathway for propionate activation in *C. glutamicum*. In addition to propionate consumption, measuring its metabolic derivatives, such as intracellular methylmalonyl-CoA and propionyl-CoA, directly showed the correlation between length of lag phase and concentrations of these CoAs (Fig. 2a and 2e). Taken together, these results show that propionate derivatives like propionyl-CoA and methylmalonyl-CoA may be the cause of growth inhibition, not free propionate itself.

2. Methylmalonyl-coa Accumulation Induces Growth Inhibition In Propionate Medium

To determine the cause of the dose-dependent growth lag in the presence of propionate, we next evaluated the propionyl-CoA metabolism. *C. glutamicum* encodes two distinct pathways for propionyl-CoA metabolism. The first is the 2-methylcitrate pathway, in which propionyl-CoA and oxaloacetate are combined to form free CoA-SH and 2-methylcitrate, which is then transformed to 2-methylisocitrate by PrpD and then to pyruvate and succinate by PrpB. An alternative is methylmalonyl-CoA pathway, which involves carboxylation of propionyl-CoA to yield (S)-methylmalonyl-CoA followed by isomerization to (R)-methylmalonyl-CoA, and then conversion to the TCA cycle intermediate succinyl-CoA to support cell growth (Fig. 3a)[28]. Transcriptomic analysis showed that the three genes (*prpD2B2C2*) encoding the 2-methylcitrate pathway were significantly up-regulated when cells were cultivated in CGXII minimal medium with 1 g/L propionate. The genes involved in the methylmalonyl-CoA pathway were up-regulated as well, but not as strongly as the 2-methylcitrate pathway (Fig. 3a). The 2-methylcitrate pathway should be favored over the methylmalonyl-CoA pathway because the Gibbs free energy (ΔrG'm) of the reaction that converts propionyl-CoA to 2-methylcitrate is negative (ΔrG'm = -40.4 ± 6.6 kj/mol), whereas that for conversion of propionyl-CoA to methylmalonyl-CoA is positive (ΔrG'm = -5 ± 10.3 kj/mol) and requires one ATP to fix CO_2 (Fig. 3a). To prove this hypothesis, the wild-type strain was cultivated in CGXII minimal medium with [^{13}C3]propionate. Analysis of pathway intermediates using LC-MS showed that more than 99% of [^{13}C3]propionate was transformed through the 2-methylcitrate pathway rather than through the methylmalonyl-CoA pathway (Extended Data Fig. S4a). All the above results indicate that the 2-methylcitrate pathway is favored over the methylmalonyl-CoA pathway to consume propionyl-CoA. To clarify whether this pathway causes growth inhibition, six genes (*cgl0657-0659* (*prpD2B2C2*) and *cgl0694-0696* (*prpD1B1BC1*)) involved in the 2-methylcitrate pathway were deleted in the wild-type strain, resulting in strain Cz05, which only retains the methylmalonyl-CoA pathway for propionyl-CoA assimilation. In CGXII minimal medium containing 1 g/L propionate, Cz05 had an even longer lag phase but showed less accumulation of methylcitrate than wild-type (Fig. 3b), indicating that 2-methylcitrate accumulation is not the cause of growth lag, and further supporting the hypothesis that growth lag is caused by accumulation of propionyl-CoA and methylmalonyl-CoA, "dead-end" CoAs with no role in primary metabolism.

We performed additional experiments to show that accumulation of these acyl-CoAs is the cause of growth inhibition in propionate. We overexpressed the gene encoding *E. coli* propionyl-CoA synthetase (*prpE*) in Cz05 to generate Cz07, the gene encoding propionyl-CoA carboxylase (*pcc*) from *S. coelicolor* to generate Cz08, or both heterologous genes to generate Cz09. Cz07, Cz08, and Cz09 grew slower than Cz05 (Fig. 3d), indicating that enhanced methylmalonyl-CoA pathway inhibits cell growth in propionate-containing medium. To clarify which CoA metabolites contribute to growth inhibition, propionyl-CoA and methylmalonyl-CoA concentrations were measured in all strains. Compared to Cz05, both propionyl-CoA and methylmalonyl-CoA concentrations were significantly increased in Cz07, Cz08 and Cz09 relative to those in Cz05 (Fig. 2d), indicating that both propionyl-CoA and methylmalonyl-CoA contribute to growth inhibition.

Further support for our acyl-CoA derivatives accumulation hypothesis comes from the fact that addition of vitamin B12 relieves growth inhibition in propionate-containing medium[35]. *C. glutamicum* harbors a vitamin B12-dependent methylmalonyl-CoA/succinyl-CoA mutase (encoded by *cgl1529-1530*), which can catalyze the reversible conversion of these two metabolites (Fig. 3a). Vitamin B12 addition provides a new outlet for converting "dead-end" methylmalonyl-CoA to succinyl-CoA, which then enters the TCA cycle to support cell growth and regenerate free CoA-SH[28]. Transcriptomic analysis showed that *cgl1529-1530* are upregulated in the presence of propionate compared to glucose only (Fig. 3a). We deleted *mcmAB* (c*gl1529-1530*) in wild-type to generate strain Cz04, with its 2-methylcitrate pathway still intact. Compared to wild-type, little or no growth inhibition was observed in Cz04 when it was cultivated in CGXII minimal medium with 1 g/L propionate (Fig. 3b), which provides further support that 2-methylcitrate accumulation does not contribute to growth inhibition in propionate medium. To confirm that vitamin B12 rescues growth by enabling conversion of methylmalonyl-CoA to succinyl-CoA, *cgl1529-1530* were deleted in Cz05 to generate Cz06 (both methylcitrate and methylmalonyl-CoA conversion pathways deleted). We compared the growth of Cz04, Cz05, Cz06 and wild-type cells in CGXII with 1 g/L propionate and 10 uM vitamin B12. Cz05 grew much faster than Cz06 (Fig. 3c) and had no lag phase compared with wild-type, indicating that enhancing methylmalonyl-CoA conversion to succinyl-CoA rescues cell growth in propionate medium. When we consider our results from evaluating (I) and (II) (Fig. 3d), we reasoned that free CoA was fixed by propionate in (I) and is released when succinyl-CoA enters the TCA cycle in (II), indicating that free CoA may be important to rescue growth in propionate-containing medium. Compared to wild-type, the free CoA concentration decreased in Cz05 and Cz06 (Extended Data Fig. S5). In addition, transcriptomic analysis showed that genes involved in *de novo* biosynthesis of free CoA were upregulated in propionate-containing medium (Extended Data Fig. 6e). To test whether free CoA is involved in propionate inhibition, the genes encoding the free CoA production pathway (aspartase from *E. coli* and aspartate 1-decarboxylase from *C. glutamicum*) were overexpressed to generate strain Cz10. Compared with Cz05, Cz10 showed a much shorter lag phase that was similar to wild type (Fig. 3e), which further supports the hypothesis that the lack of free CoA is one reason for the growth inhibition in propionate.

The above results showed that enhanced methylmalonyl-CoA conversion or CoA supplementation should rescue cell growth in propionate. To clarify which approach works better, Cz05 was cultivated in different concentrations of propionate with vitamin B12 or sodium pantothenate (precursor to coenzyme-A). Although enough sodium pantothenate was added, the lag phase increased with increasing propionate concentration. And the lag phase in sodium pantothenate was always longer than when vitamin B12 was supplemented to the medium. Compared to CoA supplementation, vitamin B12 addition works better to rescue cell growth in propionate-containing medium by conversion methylmalonyl-CoA (Extended Data Fig. S6a, b, c, and d). Taken together, these results indicated that accumulation of propionyl-CoA and methylmalonyl-CoA is the cause of growth inhibition in propionate medium, and that methylmalonyl-CoA conversion can rescue cell growth.

3. Methylmalonyl-coa Dependent Pkss Rescue Cell Growth In Propionate Medium

Since methylmalonyl-CoA is one of the most common extender units for PKSs[11] and propionyl-CoA also acts as an important starter unit for PKSs[37], increasing methylmalonyl-CoA or propionyl-CoA concentrations is a common strategy to increase polyketide production[17]. Our previous results indicated that both propionyl-CoA and methylmalonyl-CoA are involved in propionate inhibition and conversion of methylmalonyl-CoA rescues cell growth in propionate medium. Taking all these results into consideration, we hypothesized that methylmalonyl-CoA conversion could be achieved by introducing methylmalonyl-CoA-dependent PKSs, which will not only rescue cell growth in propionate but also would promote polyketide production. Based on this hypothesis, we introduced several heterologous methylmalonyl-CoA dependent PKSs (Fig. 4a).

Several genetic modifications were made to facilitate polyketide production. Phosphopantetheinyl transferases (PPTase) are required to activate acyl carrier protein (ACP) domains within PKSs. *C. glutamicum* encodes a native PPTase, so we first evaluated if heterologous expression of an additional PPTase, *sfp* from *Bacillus subtilis*, is necessary to support the native enzyme. Non-ribosomal peptide synthetase (NRPS) BpsA is an enzyme that produces a blue pigment, indigoidine[34, 38], when its carrier protein domains are phosphopantetheinylated. We overexpressed *bpsA* and showed that co-expression of *sfp* resulted in higher indigoidine production compared to the strain lacking *sfp* (Extended Data Fig. S7a). Based on these results, we moved forward with strains that overexpressed *sfp*. We then intentionally increased the accumulation of methylmalonyl-CoA by deleting the 2-methylcitrate pathway (main pathway consuming propionyl-CoA) and *cgl1529-1530* (mutase A and B) to generate Cz34 strain, which we used as the basis for subsequent PKS pathways integration.

The first PKS we tested was germicidin synthase (Gcs), a type III PKS from *Streptomyces coelicolor* that uses methylmalonyl-CoA as the extension unit to synthesize germicidin[39]. This compound has significant inhibitory activity on hexokinase (HK2, IC_{50} = 0.78 mg ml^{-1}), which is expressed at a high level in cancer cells[40]. To test whether introduction of a methylmalonyl-CoA–dependent PKS can rescue cell growth in propionate medium, the entire germicidin production pathway was introduced into Cz34 to generate Cz12 (Fig. 4a). We compared the growth of Cz34 and Cz12 in CGXII minimal medium with 600 mg/L propionate. We found that Cz12 had a shorter lag phase (decreased 75%) compared to Cz34 when grown in propionate-containing medium (Fig. 4b). The label incorporated into germicidin C when our engineered strain was grown in the presence of [^{13}C3]propionate (Extended Data Fig. S8) supports our hypothesis that the introduced germicidin production pathway is using methylmalonyl-CoA and is improving growth in propionate medium by converting methylmalonyl-CoA into a targeted product and releasing CoA-SH.

To show that this is a general phenomenon to all methylmalonyl-CoA–dependent synthases, we introduced several other heterologous PKSs into Cz34, including two type III PKSs from *Mycobacterium marinum* (Mmar_2470 and Mmar_2474)[41] and an engineered type I PKS, LipLM-M1-debsM6TE, which we

have shown to produce hydroxy acids in *Streptomyces*[22, 42]. All heterologous PKS pathways resulted in a shorter lag phase in 0.6 g/L propionate compared to Cz34 lacking a PKS pathway, although the degree of growth improvement varied between PKS pathways (Fig. 4c, Extended Data Fig. S7, 9, and 10).

To further increase germicidin titer, we cultivated the engineered strain in a minimal medium with different propionate concentrations and measured growth and germicidin production. Germicidin production increased as the propionate concentration increased, even though the lag phase also increased especially with propionate concentrations over 1 g/L (Fig. 4d and Extended Data Fig. S11). Although introduction of the germicidin PKS improved cell growth in propionate medium, the engineered strains still grew slower in propionate medium compared with cells growing without propionate. This inhibition was more severe when the propionate concentration increased beyond 1 g/L.

4. Methylmalonyl-coa Toxicity Promote Germicidin Production Pathway Evolution

To determine the highest propionate concentration for ALE, Cz034 was cultivated in CGXII minimal medium with various concentrations of propionate. The lag phase increased as the propionate concentration increased, and no growth was observed when the propionate concentration was over 8 g/L (Extended Data Fig. S11a, b). Then, ALE was applied to improve propionate tolerance and germicidin production in Cz12 by repeatedly growing the strains in increasing concentrations of propionate until we reached 8 g/L (Extended Data Fig. S12). After two months of evolution, 563 single colonies were selected from plates. Most of them grew faster than the initial strain (Extended Data Fig. S13a,b,c,d). Surprisingly, evolved strain CzEv208 (knockout methylcitrate pathway and methylmalonyl-CoA pathway) grew even faster in 8 g/L propionate than wild-type grown in CGXII minimal medium without propionate (Fig. 5a). The growth rate of CzEv208 was 140% faster than that of Cz12, and the lag phase was significantly shorter (by 80%) (Fig. 4d and Extended Data Fig. S13e,f). These results indicate that methylmalonyl-CoA turnover in CzEv208 was significantly improved. To clarify whether the increased germicidin production improved methylmalonyl-CoA utilization, germicidin titer was measured in cultures of evolved strains. Compared to Cz12, germicidin production in almost all evolved strains was significantly increased (Fig. 5b). The germicidin titer produced by CzEv208 (13.6 ± 0.05 mg/L) was 18-fold higher than that produced by Cz12 (0.78 ± 0.03 mg/L) (Fig. 5d), indicating that strains harboring beneficial mutations for germicidin production have been selected during ALE.

To determine which genetic changes in the evolved strains are correlated with improved titers and growth rates, we first sequenced all six genes involved in the germicidin production in the best performing evolved strains. Three promising mutations (L216P, T257A and R347L) were found in Gcs of the evolved strains (4 out of 6 evolved strains). To identify the locations of the mutated residues, SWISS-Model was used to model the structure of Gcs based on 3v7i.1.A (PDB)[39]. Two mutations (L216P and T257A) are adjacent to the substrate binding tunnel (cyan, Arg (276/277/280/317)), and one mutation (R347L) is close to the active site (green, Cys175-His312-Asn346) (Fig. 5c)[39]. To validate whether these mutations

were responsible for the improved germicidin production and cell growth in evolved strains, we replaced the native *gcs* gene in Cz12 with different mutant versions of the gene found in our evolved strains. Neither L261P nor T257A (singly or in combination) affected cell growth and germicidin production (Extended Data Fig. S14a and b). However, when Gcs R347L was introduced into Cz12 to generate Cz33, the lag phase decreased by 32.5% and germicidin titer increased by 337.5% compared to Cz12 (Fig. 5d). Conversely, when the mutated *gcs* gene in CzEv208 was replaced by the native *gcs* gene to generate Cz32, germicidin titer decreased 18%, although the lag phase was not significantly different in the two strains (Fig. 5d). These results indicate that we can use propionate as a selective pressure to induce beneficial mutations in methylmalonyl-CoA-dependent PKSs.

5. Evolved Citrate Synthase (Glta2)-based Methylcitrate Pathway Rescue Cell Growth By Consuming Propionyl-coa

Although replacing the native Gcs in Cz12 with the evolved Gcs improved growth in propionate, the lag phase was still longer than that of evolved strain, indicating that some other mutations may be involved in rescuing growth of the evolved strain. To clarify the mechanism, genome sequencing was performed on 19 evolved strains. In addition to those mutations in *gcs* itself, there were several other mutations in our evolved strains' genomes that could lead to improved fitness. Clusters of orthologous groups (COG) category[43] of *C. glutamicum* genes were determined using EggNog, and the distribution of total genes and SNP-containing genes in each category were compared. For the genes with SNPs, categories C (energy production and conversion) and G (carbohydrate transport and metabolism) were particularly enriched in SNPs. Citrate synthase (GltA2), which belongs to category C, was mutated in most of the evolved strains (18 out of 19 evolved strains) (Fig. 6a). To test whether SNPs in GltA2 are involved in cell growth rescue and germicidin titer increases, the mutated GltA2 in CzEv208 was replaced by the native GltA2 to generate Cz14. Compared to CzEv208, Cz14 grew much slower and germicidin production was lower (Fig. 6b). Next, we replaced the native *gltA2* in Cz12 with the evolved *gltA2* variant to generate Cz15. Cz15 grew faster than Cz12 (lag phase decreased by 37%) and germicidin titer also increased (by 318%) (Fig. 6b), indicating that the mutation in GltA2 is involved in the improved growth phenotype and germicidin production. The evolved GltA2 had three mutations: E239G, R310C, and S60F (Extended Data Fig.S15a). These mutations were individually introduced into Cz12 to generate Cz16, Cz17 and Cz18. Compared to the other two mutations, S60F (Cz18) showed the greatest impact on growth in propionate medium (Fig. 6b).

Citrate synthase is a key component of the TCA and glyoxylate cycles. The latter pathway is closely analogous to the methylcitrate pathway in that the substrates (acetyl-CoA and propionyl-CoA) and products (glyoxylate and pyruvate) differ by a single methyl group. We therefore hypothesized that the evolved mutations in GltA2 resulted in an improved ability to accept propionyl-CoA as a substrate. To directly test this hypothesis, the native GltA2 and GltA2 S60F were purified (Extended Data Fig.S15b). *In vitro* citrate synthase kinetic assays showed that the evolved GltA2 S60F had higher activity for propionyl-CoA compared to the native GltA2(Fig. 6c). Transcriptomic data showed that the genes encoding

isocitrate lyase (*aceA*) and malate synthase (*aceB*) were upregulated in our evolved strains (CzEv231, CzEv236, CzEv261) compared to parental strain Cz12. We hypothesize that the evolved strains mutated S60F mutation of GltA2 to accept propionyl-CoA as a substrate and increased expression of the native *aceA*, evolved a new methylcitrate cycle in *C. glutamicum* from its endogenous glyoxylate cycle (Fig. 6e). To test whether the evolved methylcitrate pathway is involved in propionate rescue, we deleted *aceA* and *aceB* in CzEv208 to generate Cz20. Compared to CzEv208, Cz20 had a longer lag phase and produced less germicidin (Fig. 6d), which indicated that evolved *gltA2* and overexpressed aceA/B are all involved in the evolved methylcitrate pathway.

To clarify which pathway (methylmalonyl-CoA pathway or evolved methylcitrate pathway) consumes more propionate in the evolved strain, the evolved strain was cultivated in minimal medium with [$^{13}C_3$]propionate. The most abundant product, germicidin C, was derived from the methylmalonyl-CoA pathway (germicidin C only labeled by methylmalonyl-CoA ($MS[H + H]^+ = 186$)), not from the evolved methylcitrate pathway (germicidin C labeled by methylmalonyl-CoA and 2-methylbutyryl-CoA ($MS[H + H]^+ = 188$)) (Fig. 6e and Extended Data Fig. S16). This result indicates that propionyl-CoA was primarily converted to methylmalonyl-CoA in CzEv208 and does not enter the evolved methylcitrate pathway. The evolved methylcitrate pathway activity is not comparable to a native methylcitrate pathway.

In addition to GltA2, the COG analysis results also showed that category G (carbohydrate metabolism and transport) was enriched. One of the category G genes, *bmr3* (*cgl038*0), encodes a permease of major facilitator superfamily transporter. We deleted *bmr3* in CzEv208, which had a significantly increased the lag phase. Overexpression of evolved *bmr*3 in Cz12 generated Cz42, and this change rescued cell growth in propionate-containing medium (Fig. 6d), indicating that *bmr*3 is also involved in propionate rescue. To test this hypothesis, propionate consumption was measured in wild-type, Cz12, CzEv208, Cz41(*bmr3* deleted in CzEv208) and Cz42 (evolved *bmr*3 overexpressed in Cz12). Cz42 consumed more propionate than Cz12 ($p = 0.068 > 0.05$), whereas Cz41 consumed less propionate than CzEv208 ($p = 0.068 > 0.05$). Cz41 and Cz42 consumed relatively similar amounts of propionate (Extended Data Fig. S18).

Discussion

Our study revealed that addition of propionate to minimal medium leads to growth inhibitory levels of propionyl- and methylmalonyl-CoA in *C. glutamicum* and demonstrated that we can leverage this growth inhibition as a selective pressure to evolve strains to improve growth and polyketide production. We expressed several different PKS systems to relieve the growth inhibition in *C. glutamicum*, and in all cases polyketide production was correlated with faster growth in propionate, demonstrating that this strategy can be applied generally.

We used germicidin synthase as an example to demonstrate the utility of this system for improving polyketide production through evolution. Some of the strains showing improved growth harbored beneficial mutations in the PKS gene that improved the activity of the enzyme. However, mutations arising elsewhere in the genome were much more common than mutations in the PKS gene itself.

Compared to the size of the host's genome PKSs are small, so there will be statistically fewer mutations in PKSs. Additionally, other mechanisms for dealing with the accumulation of propionyl-CoA and methylmalonyl-CoA needed to be activated to deal with this stress. For example, although *gltA2* and *prpC* showed significant sequence similarities, native GltA*2* did not have methylcitrate synthase activity[28]. Mutations in *gltA2*, which turned it into a methylcitrate synthase needed for a glyoxalate cycle, occurred in most of the evolved strains. When we replaced the native *gltA2* with evolved *gltA2* in Cz12, the evolved enzyme relieved growth inhibition in propionate-containing medium. When we replaced the evolved *gltA2* in CzEv208 with the native *gltA2*, the lag phase increased (Fig. 6b). Using *in vitro* citrate synthase assays, we confirmed that evolved GltA2 has higher activity with propionyl-CoA compared to native GltA2. The mutations that occurred in *gltA2* led to the emergence of an evolved methylcitrate pathway to rescue cell growth in propionate such that mutant GltA2 can now perform the same function as a promiscuous methylcitrate synthase. This novel pathway can then relieve propionate inhibition by consuming propionyl-CoA and releasing free CoA (Fig. 3a), similar to the native methylcitrate pathway.

Another example of a beneficial mutation that occurred outside the PKS gene was discovered in *bmr3* (*cgl0380*), which also relieved propionate inhibition. COG category analysis showed that *bm3* belongs to category G, suggesting that *bmr3* may encode a membrane protein that is involved in propionate transport. Blast results showed that Bmr3 is a permease belonging to the major facilitator superfamily, proteins that facilitate movement of small solutes across cell membranes in response to chemiosmotic gradients. Mutations in membrane proteins therefore represent another way for the cells to circumvent propionate growth inhibition, and these types of proteins should be accounted for in future engineering efforts.

PKSs have promising commercial value for production of a variety of chemicals, but heterologous production of polyketides faces significant challenges, including host engineering[44–46], precursor supplementation[12, 15, 47] and improvement of PKSs activity[48–50]. Generally, the titer, production rate, and yield of a desired polyketide, particularly those produced by hybrid (non-natural) PKSs, are too low for commercial viability of anything but expensive pharmaceutical ingredients. Because there are few screening/selection methods for improving PKSs, PKS engineering has generally relied on rational design, which requires significant knowledge about protein structure and the interactions of domains and modules[51]. Most previous polyketide production improvements have focused on precursor supply[52, 53] or low-throughput analytical chemistry-based screening of engineered PKSs (e.g. chromatography and mass spectrometry)[54, 55]. Here, we demonstrated that PKSs could be evolved to have improved activity using a strain that accumulates polyketide precursors that are inhibitory to cell growth. Without much work, we were able to evolve a polyketide synthase, Gcs, to have higher activity compared to the native Gcs, thereby increasing the final product titer 18-fold. Although a vast majority of the mutations in the evolved strains were not in the target PKS gene, future evolution experiments could employ directed evolution strategies to introduce much more mutations in the PKS gene(s)[56]. The ability to screen and select improved polyketide producers by growing in propionate will greatly improve the ease and rate, which lead us study these complex biosynthetic enzymes.

Declarations

Acknowledgements:

This work was part of the DOE Joint BioEnergy Institute (jbei.org) supported by the U.S. Department of Energy, Office of Science, Office of Biological and Environmental Research, through contract DE-AC02-05CH11231 between Lawrence Berkeley National Laboratory and the U.S. Department of Energy. The views and opinions of the authors expressed herein do not necessarily state or reflect those of the United States Government or any agency thereof. Neither the United States Government nor any agency thereof, nor any of their employees, makes any warranty, expressed or implied, or assumes any legal liability or responsibility or the accuracy, completeness, or usefulness of any information, apparatus, product, or process disclosed or represents that its use would not infringe privately owned rights. The United States Government retains and the publisher, by accepting the article for publication, acknowledges that the United States Government retains a nonexclusive, paid-up, irrevocable, worldwide license to publish or reproduce the published form of this manuscript, or allow others to do so, for United States Government purposes. The Department of Energy will provide public access to these results of federally sponsored research in accordance with the DOE Public Access Plan (http://energy.gov/downloads/doe-public-access-plan). Funding for open access charge: US Department of Energy.

Conflicts of Interest:

J.D.K. has financial interests in Amyris, Ansa Biotechnologies, Apertor Pharma, Berkeley Yeast, Cyklos Materials, Demetrix, Lygos, Napigen, ResVita Bio, and Zero Acre Farms.

Data availability

The accession number for the genome sequence data of evolved strains reported in this paper is [NCBI.SAMN]: [PRJNA893829]. All RNA-seq data were attached to Supplementary.

Materials And Methods

Strains and reagents. Plasmids and strains are listed in Supplemental Data Table 1 (https://public-registry.jbei.org/folders/763). Phusion polymerase and HiFi DNA Assembly kits were purchased from New England Biolabs, Fast Digest restriction enzymes were purchased from Thermo Scientific. All oligonucleotides were synthesized at Integrated DNA Technologies (IDT). Germicidin C standard was synthesized by Wuxi ApTec (Tianjin). Sodium [$^{13}C_3$]propionate was purchased from Cambridge Isotope

Laboratories (USA). All other chemicals were purchased from Sigma-Aldrich. All codon optimized heterologous genes were synthesized by GenScript and are listed in Supplemental Data Note 1.

Competent cell preparation and electrotransformation. *C. glutamicum* competent cells were first cultivated in BHI (37 g Brain Heart Infusion powder in 1 L H_2O) liquid medium overnight (30 ℃, 200 rpm). Then cells were inoculated into EPO medium (37 g BHI, 25 g Glycine, 10 mL Tween, 4 g Isoniazid), 30 ℃, 200 rpm for 5-6 hours until the OD_{600} was approximately 1.0. Cells were washed three times with ice cold 10% glycerol and resuspended in 1 mL ice cold 10% glycerol. 80 µl of these competent cells were transformed with 500 ng episomal plasmid in ice-cold electroporation cuvettes (0.2 cm gap). After electroporation, cells were resuspended in 1 mL of liquid BHI media, heat shocked at 46 ℃ for 5 minutes, and then incubated at 30 ℃ for 1-2 hours. Cells were plated on BHI + 25 µg/mL kanamycin for 2 days. Single colonies were streaked on BHI + 10% Sucrose plates and incubated at 30 ℃ for 1-2 days to loop out the selection marker. Colonies were then picked and verified by colony PCR.

Colony PCR. Picked colonies were cultivated in BHI medium (30 ℃, 200 rpm) overnight (around 14-16h). Digestion solution was prepared by adding 120 µL zymolyase (E1005, ZYMO RESEARCH) to 2500 µL phosphate buffed saline (PBS) pH = 7.2 for 96 reactions. 3-5 µL of overnight culture was then mixed with 20 µL digestion solution and incubated at 30 ℃ for 1h. 3-5 µL of dimethyl sulfoxide (DMSO) was then added and the mixture was heated at 98 ℃ for 10min. 2 µL of this mixture was used as template for 50 µL colony PCR reactions.

Growth curve measurements. Cells were pre-cultivated in BHI liquid medium (30 ℃, 200 rpm) overnight. Cells were inoculated into CGXII minimal medium (20 µL culture into 2 mL medium) and incubated at 30 ℃, 200 rpm for 16-18 h. Then cells were inoculated into 48 well assay plates containing fresh CGXII minimal medium with or without propionate (original OD_{600} is around 0.1). OD_{600} was measured using a SpectraMaX M2e plate reader at 30 ℃.

[$^{13}C_3$] label experiments. For all experiments using [$^{13}C_3$]propionate as a media component, strains were pre-cultivated in BHI liquid medium (30 ℃, 200 rpm) overnight. Cells were inoculated into CGXII minimal medium and grown (30 ℃, 200 rpm) for 8-12 h. Then cells were subcultured into fresh CGXII minimal medium with 1 g/L [$^{13}C_3$]propionate (99.0% atom enrichment, Cambridge Isotope Laboratories, USA). For metabolites or CoA measurement, cells were collected during the early exponential phase (OD_{600} 0.8-1.2). For targeted chemical measurement, cells were collected at stationary phase.

Metabolite extraction and measurement. Strains were collected during the early exponential phase. The culture was centrifuged at 4 ℃, 5000 × g for 10 min. Cell pellets were stored at -80 ℃. Cells (8 mg of dried cells is equal to approximately 2 mL of OD_{600} = 2 culture) and supernatant were mixed with acetonitrile/methanol/50 mM formic acid (45:45:10, v/v) containing 5 nM [^{13}C]malonyl-CoA (internal standard) to a final volume of 1 mL. The extraction was performed on ice with intermittent vortexing for

15 minutes, followed by a 3-minute centrifugation at 13,000 × g and 4 ℃. The supernatant was freeze dried, and metabolites were resuspended in 100 µL resuspension buffer (50 mM ammonium formate, pH 3.0, 2% methanol)[37]. Liquid chromatography-mass spectrometry (LC-MS) was used to analyze metabolite profiles as described previously[57, 58].

LC-MS measurement of Germicidin C. 0.5 mL culture was centrifuged at 13,000 × g, 4 ℃ for 10 min. 200 µL methanol was then mixed with 200 µL supernatant. Samples were filtered using 3-KDa filter plates (PALL, Omega 3K). Cell pellets were resuspended using 0.5 mL methanol and samples were mixed in an Eppendorf Thermomixer R Mixer (23 ℃, 1000 rpm) overnight (around 12-14h). 0.5 mL ddH_2O was added into samples, and all samples were filtered using 3-KDa plate (PALL, Omega 3K). LC-MS analyses were performed on the LC-MSD iQ system with a mass selective detector (Agilent). 2 µL of samples were loaded onto the Kinete®XB-C18 column (2.6 µm, 100 × 3 mm, Phenomenex) at a flow rate of 0.425 mL/min at 45 ℃: 0 to 5.0 min, 80% mobile phase A (0.1% formic acid in water)/20% mobile B (0.1% formic acid in methanol); 5.0 min to 6.0 min, gradient from 51.8% mobile phase A /48.2% mobile B to 5.0% mobile phase A/95% mobile B; 6.0 min to 9.0 min, 5% mobile phase A /95% mobile B ; 9.0 min to 9.1 min, gradient from 5% mobile phase A/95% mobile B to 80% mobile phase A/20% mobile B. 9.1 min to 12.0 min, 80% mobile phase A/20% mobile B.

HPLC measurement of propionate. Culture was centrifuged 13,000 × g for 10 min at 4 ℃. 100 µL supernatant was added into 100 µL 5 mM H_2SO_4. Samples were filtered using 3-KDa plate (PALL, Omega 3K). HPLC analysis was performed on the HPLC (Agilent 1200 series) equipped with a diode array detector (DAD) and refractive index detector (RID), which were used to detect propionate. 5 µL of different samples were loaded onto the using HPX-87H (Bio-Rad) at a flow rate of 0.5 mL/min at 65 ℃.

Protein purification. pET-LIC-Cgl2569, pET-LIC-GltA2 wild-type and pET-LIC-GltA2 mutation were transformed into BL21(DE3) competent cells. Single colonies of each were picked from LB + 50 µg/mL kanamycin plates and cultivated in 5 mL LB + 50 µg/mL kanamycin liquid medium overnight at 37 ℃, 200 rpm. 2 mL overnight culture was used to inoculate into 500 mL Terrific Broth containing 4% glycerol (6 g tryptone, 12 g yeast extract, 20 mL glycerol with 500 mL H_2O) in a 2-L baffled culture flask. Cells were grown at 37 ℃, 200 rpm until OD_{600} reached 0.6 - 1.0. The flask was transferred to 20 ℃ with shaking for 1 h before 0.1 mM IPTG induction. The cells were harvested after additional 18-20 h incubation at 20 ℃, 200 rpm. Culture was centrifuged at 4 ℃, 4,000 rpm for 30 min to pellet cells and the pellets were stored at -20C. Cells were re-suspended in 50 mL Lysis Buffer (300 mM NaCl, 25 mM Tris pH 7.5 and 10% glycerol) and vortexed 30 min at 25 ℃, then placed on ice. Cells were lysed with sonication (30 s on then 60 s off, repeated 6 times). Lysate was cleared by centrifugation at 17000 × g for at least 30 min, followed by 0.45-um membrane filtration to collect supernatants. Ni affinity chromatography was used for protein purification. Filtered supernatants were loaded onto a 5 mL His-Trap column at 3 mL/min flow rate, followed by 50 mL 300 mM NaCl, 25 mM Tris pH 7.5, 20 mM imidazole pH 7.5, and 10% glycerol wash at 4 mL/min flow rate. The His-tagged protein was eluted with 300 mM NaCl, 25 mM Tris pH 7.5, 500 mM imidazole pH 7.5, and 10% glycerol at 4 mL/min flow rate and 30 mM/min imidazole gradient.

Collected fractions were analyzed by SDS-PAGE, confirming > 90% homogeneity. Fractions containing the target protein were dialyzed in 1 L storage buffer (100 mM NaCl, 25 mM Tris pH 7.5 and 10% glycerol) at 4 ℃ overnight, concentrated to 3.0 mg/mL final protein concentration, and stored at -80 ℃.

In vitro assay to measure Cg2569 activity. We first prepared 10 mM stock solutions of acyl-CoAs. We then mixed 0.2 mM acyl-CoA (eg. succinyl-CoA) with 0.2 mM acid (e.g., propionate) and purified Cg2569 protein in100 µL PBS (pH = 7.4). Reactions were incubated at room temperature for 20 min[38]. Then 100 µL methanol was added into the reaction system and samples were centrifuged at 4 ℃. The solutions were filtered with 3-KDa columns and 50 µL filtered sample was used for LC-MS measurement (A common approach for absolute quantification of short chain CoA thioesters in prokaryotic and eukaryotic microbes). All samples were run in duplicate.

In vitro assay to measure citrate synthase activity. We followed the citrate synthase activity assay kit protocol (Catalog Number MAK193, SIGMA-ALDRICH) with minor modifications. 5 µmol purified citrate synthase was added into reaction system, containing 6.4 µl 50 mM DNTB, 10 µl 20 mM oxaloacetate and different concentrations of acetyl-CoA or propionyl-CoA (0 µM, 100 µM, 200 µM, 300 µM, 400 µM and 500 µM) in 200 µl reactions. Reactions were incubated at 25 ℃ for 20 min. Absorbance at 412 nm was measured using SPMAX-384PLUS plate reader every 9 s. All samples were run in duplicate.

Whole genome sequencing and data analysis. Strains were cultivated in BHI liquid medium overnight (30 ℃, 200 rpm). 20 µl culture was transferred into CGXII minimal medium (30 ℃, 200 rpm) for 16h. Then 20 µl culture was transferred into CGXII minimal medium with 8 g/L propionate medium (30 ℃, 200 rpm) for 32 hours or 120 hours for initial strains. Cells were pelleted and stored at - 80 ℃. Genomic DNA was isolated using Wizard® Genomic DNA Purification Kit. 100 ng of gDNA was sheared to 600 bp using the fragmentation enzyme in xGen™ DNA Lib Prep EZ kit (Integrated DNA Technologies, Inc) and size selected using SPRI beads (Beckman Coulter). The fragments were treated with end-repair, A- tailing, and ligation of Illumina compatible adapters (Integrated DNA Technologies, Inc) using the xGen™ DNA Lib Prep EZ kit. Bioanalyzer High Sensitivity DNA Kit (Agilent) and Qubit Fluorometers (ThermoFisher Scientific) were used to determine the concentration of the libraries. Libraries were sequenced on the Illumina Miseq.

Transcriptome profiling. Strains were cultivated in BHI liquid medium overnight (30 ℃, 200 rpm). 20 µl culture was transferred into CGXII minimal medium (30 ℃, 200 rpm) for 16h. Then 20 µl culture was transferred into CGXII minimal medium with 8 g/L propionate medium (30 ℃, 200 rpm) for 12 h (OD_{600} is around 0.8) or 70 h (OD_{600} is around 0.8) for initial strains. Total RNA was extracted by GENEWIZ. The raw reads from each sample and analysis of differential expression were completed and provided by GENEWIZ. GO enrichment analysis was performed using the Platform for Integrative Analysis of Omics (PIANO) R package. COG term information was obtained from the EggNog[43]. Differential expression levels (log2-fold change) and corresponding significance levels (P values) of genes were determined by comparing evolved strains with initial strain. COG terms were calculated and scored by modulation of the expression level of genes within the same COG term.

References

1. Moore, B.S. & Hopke, J.N. Discovery of a new bacterial polyketide biosynthetic pathway. Chembiochem **2**, 35–38 (2001).
2. Smith, C.J. et al. Novel polyketide metabolites from a species of marine fungi. J Nat Prod **63**, 142–145 (2000).
3. Mapari, S.A. et al. Exploring fungal biodiversity for the production of water-soluble pigments as potential natural food colorants. Curr Opin Biotechnol **16**, 231–238 (2005).
4. Flores-Sanchez, I.J. & Verpoorte, R. Plant polyketide synthases: a fascinating group of enzymes. Plant Physiol Biochem **47**, 167–174 (2009).
5. Doull, J.L., Ayer, S.W., Singh, A.K. & Thibault, P. Production of a novel polyketide antibiotic, jadomycin B, by Streptomyces venezuelae following heat shock. J Antibiot (Tokyo) **46**, 869–871 (1993).
6. Bangera, M.G. & Thomashow, L.S. Identification and characterization of a gene cluster for synthesis of the polyketide antibiotic 2,4-diacetylphloroglucinol from Pseudomonas fluorescens Q2-87. J Bacteriol **181**, 3155–3163 (1999).
7. Piao, S.J. et al. Hippolachnin A, a new antifungal polyketide from the South China Sea sponge Hippospongia lachne. Org Lett **15**, 3526–3529 (2013).
8. Shi, Y.M. et al. Georatusin, a Specific Antiparasitic Polyketide-Peptide Hybrid from the Fungus Geomyces auratus. Org Lett **20**, 1563–1567 (2018).
9. Ratnayake, R., Lacey, E., Tennant, S., Gill, J.H. & Capon, R.J. Kibdelones: novel anticancer polyketides from a rare Australian actinomycete. Chemistry **13**, 1610–1619 (2007).
10. Hong, H., Demangel, C., Pidot, S.J., Leadlay, P.F. & Stinear, T. Mycolactones: immunosuppressive and cytotoxic polyketides produced by aquatic mycobacteria. Nat Prod Rep **25**, 447–454 (2008).
11. Keatinge-Clay, A.T. The Uncommon Enzymology of Cis-Acyltransferase Assembly Lines. Chem Rev **117**, 5334–5366 (2017).
12. Zha, W., Rubin-Pitel, S.B., Shao, Z. & Zhao, H. Improving cellular malonyl-CoA level in Escherichia coli via metabolic engineering. Metab Eng **11**, 192–198 (2009).
13. Enjalbert, B., Millard, P., Dinclaux, M., Portais, J.C. & Letisse, F. Acetate fluxes in Escherichia coli are determined by the thermodynamic control of the Pta-AckA pathway. Sci Rep **7**, 42135 (2017).
14. Takamura, Y. & Nomura, G. Changes in the intracellular concentration of acetyl-CoA and malonyl-CoA in relation to the carbon and energy metabolism of Escherichia coli K12. J Gen Microbiol **134**, 2249–2253 (1988).
15. Milke, L. & Marienhagen, J. Engineering intracellular malonyl-CoA availability in microbial hosts and its impact on polyketide and fatty acid synthesis. Appl Microbiol Biotechnol **104**, 6057–6065 (2020).
16. Mattozzi, M., Ziesack, M., Voges, M.J., Silver, P.A. & Way, J.C. Expression of the sub-pathways of the Chloroflexus aurantiacus 3-hydroxypropionate carbon fixation bicycle in E. coli: Toward horizontal transfer of autotrophic growth. Metab Eng **16**, 130–139 (2013).

17. Gonzalez-Garcia, R.A., Nielsen, L.K. & Marcellin, E. Heterologous production of 6-deoxyerythronolide B in Escherichia coli through the Wood Werkman Cycle. Metabolites **10**, 228 (2020).
18. Haller, T., Buckel, T., Rétey, J. & Gerlt, J.A. Discovering new enzymes and metabolic pathways: conversion of succinate to propionate by Escherichia coli. Biochemistry **39**, 4622–4629 (2000).
19. Murli, S., Kennedy, J., Dayem, L.C., Carney, J.R. & Kealey, J.T. Metabolic engineering of Escherichia coli for improved 6-deoxyerythronolide B production. J Ind Microbiol Biotechnol **30**, 500–509 (2003).
20. Agrimi, G. et al. Deletion or overexpression of mitochondrial NAD + carriers in Saccharomyces cerevisiae alters cellular NAD and ATP contents and affects mitochondrial metabolism and the rate of glycolysis. Applied and environmental microbiology **77**, 2239–2246 (2011).
21. Boghigian, B.A., Zhang, H. & Pfeifer, B.A. Multi-factorial engineering of heterologous polyketide production in Escherichia coli reveals complex pathway interactions. Biotechnology and bioengineering **108**, 1360–1371 (2011).
22. Yuzawa, S. et al. Short-chain ketone production by engineered polyketide synthases in Streptomyces albus. Nat Commun **9**, 4569 (2018).
23. Risdian, C., Mozef, T. & Wink, J. Biosynthesis of Polyketides in Streptomyces. Microorganisms **7** (2019).
24. Cruz-Morales, P. et al. Biosynthesis of polycyclopropanated high energy biofuels. Joule **6**, 1590–1605 (2022).
25. Weber, T., Welzel, K., Pelzer, S., Vente, A. & Wohlleben, W. Exploiting the genetic potential of polyketide producing streptomycetes. J Biotechnol **106**, 221–232 (2003).
26. Lee, N. et al. Synthetic Biology Tools for Novel Secondary Metabolite Discovery in Streptomyces. J Microbiol Biotechnol **29**, 667–686 (2019).
27. Sano, C. History of glutamate production. Am J Clin Nutr **90**, 728S-732S (2009).
28. Claes, W.A., Puhler, A. & Kalinowski, J. Identification of two prpDBC gene clusters in Corynebacterium glutamicum and their involvement in propionate degradation via the 2-methylcitrate cycle. J Bacteriol **184**, 2728–2739 (2002).
29. Huser, A.T. et al. Development of a Corynebacterium glutamicum DNA microarray and validation by genome-wide expression profiling during growth with propionate as carbon source. J Biotechnol **106**, 269–286 (2003).
30. Kirchner, O. & Tauch, A. Tools for genetic engineering in the amino acid-producing bacterium Corynebacterium glutamicum. J Biotechnol **104**, 287–299 (2003).
31. Nešvera, J. & Pátek, M. Tools for genetic manipulations in Corynebacterium glutamicum and their applications. Applied microbiology and biotechnology **90**, 1641–1654 (2011).
32. Portevin, D. et al. A polyketide synthase catalyzes the last condensation step of mycolic acid biosynthesis in mycobacteria and related organisms. Proc Natl Acad Sci U S A **101**, 314–319 (2004).
33. Lee, J.Y., Park, J.S., Kim, H.J., Kim, Y. & Lee, H.S. Corynebacterium glutamicum whcB, a stationary phase-specific regulatory gene. FEMS Microbiol Lett **327**, 103–109 (2012).

34. Plassmeier, J., Barsch, A., Persicke, M., Niehaus, K. & Kalinowski, J. Investigation of central carbon metabolism and the 2-methylcitrate cycle in Corynebacterium glutamicum by metabolic profiling using gas chromatography–mass spectrometry. Journal of biotechnology **130**, 354–363 (2007).
35. Botella, L., Lindley, N.D. & Eggeling, L. Formation and metabolism of methylmalonyl coenzyme A in Corynebacterium glutamicum. J Bacteriol **191**, 2899–2901 (2009).
36. Veit, A. et al. Pathway identification combining metabolic flux and functional genomics analyses: acetate and propionate activation by Corynebacterium glutamicum. J Biotechnol **140**, 75–83 (2009).
37. Park, Y.K., Ledesma-Amaro, R. & Nicaud, J.M. De novo Biosynthesis of Odd-Chain Fatty Acids in Yarrowia lipolytica Enabled by Modular Pathway Engineering. Front Bioeng Biotechnol **7**, 484 (2019).
38. Pang, B. et al. Investigation of indigoidine synthetase reveals a conserved active-site base residue of nonribosomal peptide synthetase oxidases. Journal of the American Chemical Society **142**, 10931–10935 (2020).
39. Chemler, J.A. et al. Biochemical and structural characterization of germicidin synthase: analysis of a type III polyketide synthase that employs acyl-ACP as a starter unit donor. J Am Chem Soc **134**, 7359–7366 (2012).
40. Bai, Y. et al. Structure-based molecular networking for the target discovery of novel germicidin derivatives from the sponge-associated streptomyces sp. 18A01. J Antibiot (Tokyo) (2021).
41. Parvez, A. et al. Novel Type III Polyketide Synthases Biosynthesize Methylated Polyketides in Mycobacterium marinum. Sci Rep **8**, 6529 (2018).
42. Yuzawa, S., Kim, W., Katz, L. & Keasling, J.D. Heterologous production of polyketides by modular type I polyketide synthases in Escherichia coli. Curr Opin Biotechnol **23**, 727–735 (2012).
43. Huerta-Cepas, J. et al. eggNOG 5.0: a hierarchical, functionally and phylogenetically annotated orthology resource based on 5090 organisms and 2502 viruses. Nucleic acids research **47**, D309-D314 (2019).
44. Wang, G., Kell, D.B. & Borodina, I. Harnessing the yeast Saccharomyces cerevisiae for the production of fungal secondary metabolites. Essays Biochem **65**, 277–291 (2021).
45. Kao, C.M., Katz, L. & Khosla, C. Engineered biosynthesis of a complete macrolactone in a heterologous host. Science **265**, 509–512 (1994).
46. Kealey, J.T., Liu, L., Santi, D.V., Betlach, M.C. & Barr, P.J. Production of a polyketide natural product in nonpolyketide-producing prokaryotic and eukaryotic hosts. *Proceedings of the National Academy of Sciences* **95**, 505–509 (1998).
47. Metz, J.G. et al. Production of polyunsaturated fatty acids by polyketide synthases in both prokaryotes and eukaryotes. Science **293**, 290–293 (2001).
48. Nivina, A., Yuet, K.P., Hsu, J. & Khosla, C. Evolution and Diversity of Assembly-Line Polyketide Synthases. Chem Rev **119**, 12524–12547 (2019).
49. Ridley, C.P., Lee, H.Y. & Khosla, C. Evolution of polyketide synthases in bacteria. Proc Natl Acad Sci U S A **105**, 4595–4600 (2008).

50. Helfrich, E.J.N. et al. Evolution of combinatorial diversity in trans-acyltransferase polyketide synthase assembly lines across bacteria. Nat Commun **12**, 1422 (2021).
51. Klaus, M. & Grininger, M. Correction: Engineering strategies for rational polyketide synthase design. Nat Prod Rep **38**, 1409 (2021).
52. Chen, D. et al. Improvement of FK506 production in Streptomyces tsukubaensis by genetic enhancement of the supply of unusual polyketide extender units via utilization of two distinct site-specific recombination systems. Applied and environmental microbiology **78**, 5093–5103 (2012).
53. Li, S., Li, Z., Pang, S., Xiang, W. & Wang, W. Coordinating precursor supply for pharmaceutical polyketide production in Streptomyces. Current Opinion in Biotechnology **69**, 26–34 (2021).
54. Ladner, C.C. New Strategies for Engineering the Substrate Specificity of Polyketide Synthases. (2016).
55. Bergmann, S. et al. Genomics-driven discovery of PKS-NRPS hybrid metabolites from Aspergillus nidulans. Nature chemical biology **3**, 213–217 (2007).
56. Yi, X., Khey, J., Kazlauskas, R.J. & Travisano, M. Plasmid hypermutation using a targeted artificial DNA replisome. Sci Adv **7** (2021).
57. Kim, J. et al. Engineering Saccharomyces cerevisiae for isoprenol production. Metab Eng **64**, 154–166 (2021).
58. Baidoo, E.E.K., Wang, G., Joshua, C.J., Benites, V.T. & Keasling, J.D. Liquid Chromatography and Mass Spectrometry Analysis of Isoprenoid Intermediates in Escherichia coli. Methods Mol Biol **1859**, 209–224 (2019).

Figures

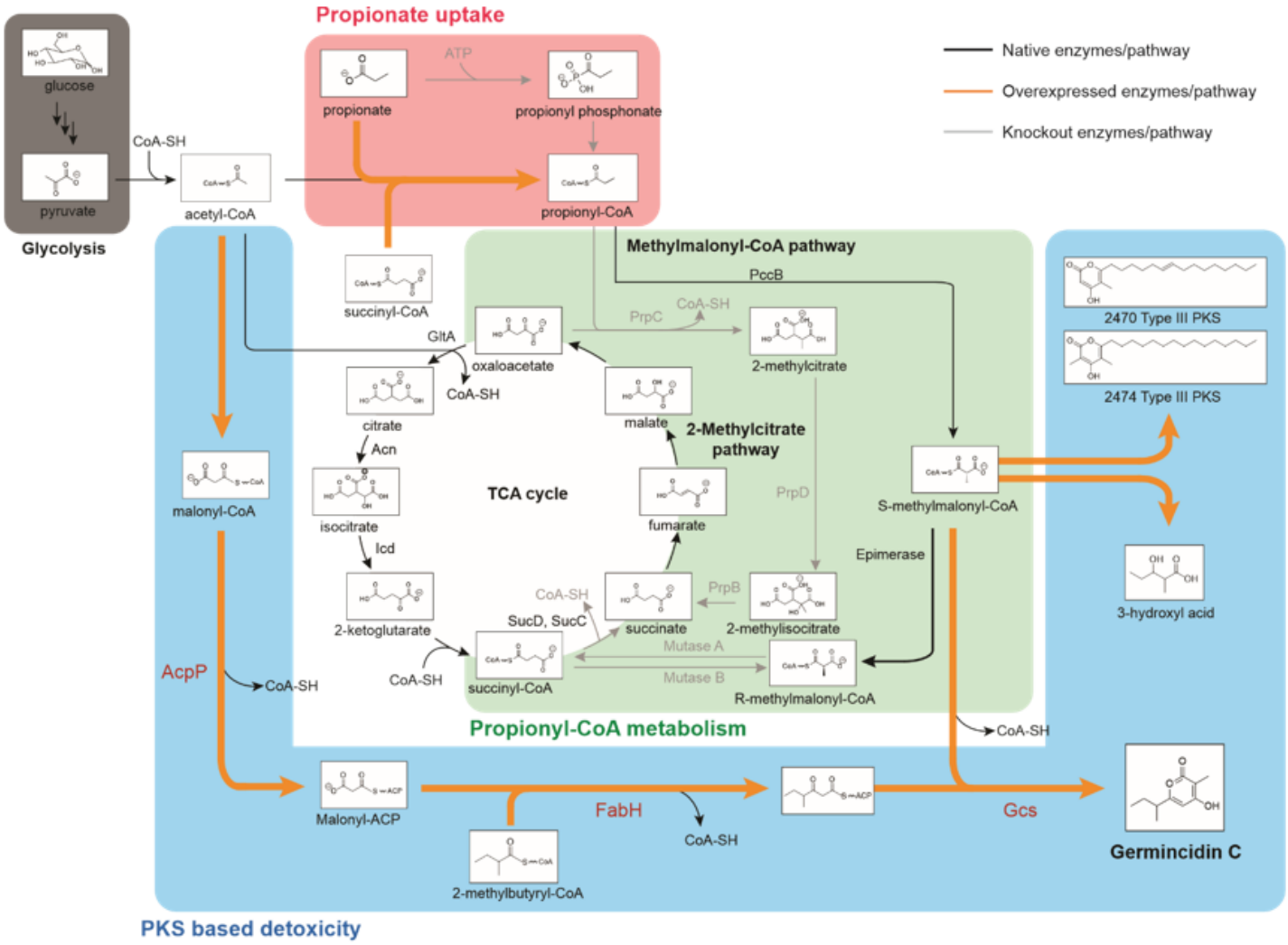

Figure 1

Propionate metabolism in *C. glutamicum.* Propionate uptake and activation to propionyl-CoA is shown in pink. Propionyl-CoA assimilation and conversion to primary metabolites is shown in green. *C. glutamicum* encodes methylcitrate and methylmalonyl-CoA pathways, both of which are shown. Polyketide production and utilization of acyl-CoAs are shown in blue. Several methylmalonyl-CoA-dependent PKSs were tested to consume methylmalonyl-CoA and relieve growth inhibition. Black lines represent native enzymes, orangelines represent overexpressed enzymes and gray lines represent enzymes that have been deleted.

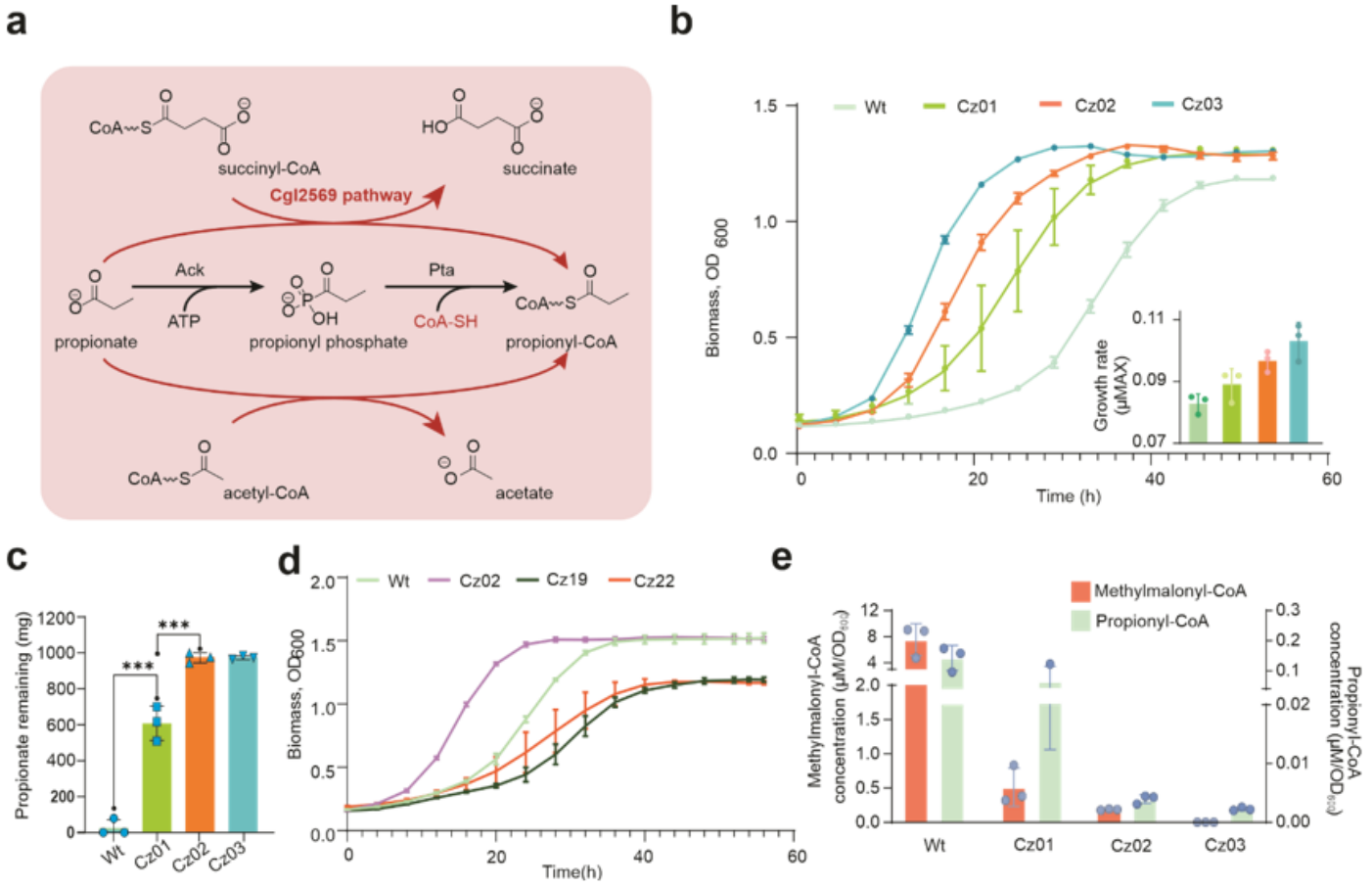

Figure 2

Propionate derivatives induce growth inhibition. a: Two pathways for converting propionate to propionyl-CoA. Cgl2569 can use either succinyl-CoA or acetyl-CoA as a substrate. b: Growth curves of wild-type and engineered propionate uptake strains in CGXII minimal medium with 1 g/L propionate: Cz01 (Δ*pta-ack*), Cz02 (Δ*cgl2569*), Cz03 (Δ*cgl2569*Δ*pta-ack*). Inset shows maximum specific growth rate for each strain. c: Propionate consumed by the four strains. d: Growth curves of wild-type and Cgl2569 overexpressing strains in CGXII minimal medium with 1 g/L propionate: Cz19 (Cgl2569 overexpressed in wild-type), Cz22 (Cgl2569 overexpressed in Cz02). e: Intracellular propionyl-CoA and methylmalonyl-CoA concentrations in the four strains. All data represents the mean ± SD, and error bars indicate the standard error (n = 3), *p < 0.05; **p < 0.05; ***p < 0.05.

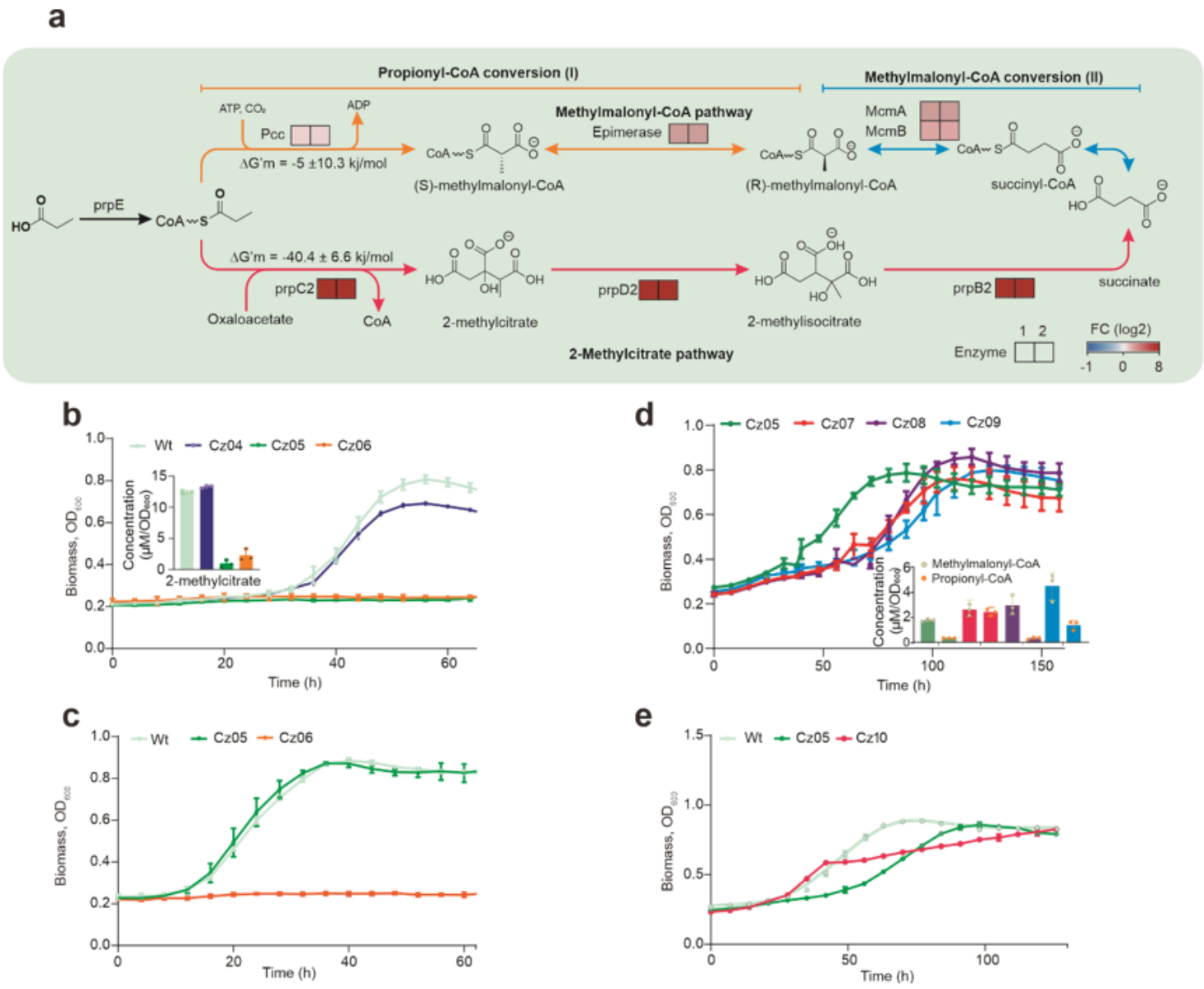

Figure 3

Accumulation of propionyl-CoA and methylmalonyl-CoA induces growth inhibition in propionate-containing media. a: Propionyl-CoA metabolism includes two pathways: (i) 2-methylcitrate pathway (pink) and (ii) methylmalonyl-CoA pathway (orange and blue). Colored boxes by the enzyme names indicate the levels of transcripts for two replicate experiments. b: Growth of various strains in CGXII minimal medium with 1 g/L propionate. Inset shows 2-methylcitrate concentration for each strain. c: Growth of various mutants in CGXII minimal medium with 1 g/L propionate and 10 μM vitamin B12. d: Growth of strains overexpressing *prpE and pcc* grown in CGXII minimal medium with 1 g/L propionate. Inset shows propionyl-CoA and methylmalonyl-CoA concentrations for each strain. e: Growth of CoA-engineered strains in CGXII minimal medium with 0.6 g/L propionate. Cz04 (*ΔmcmAB*), Cz05 (*ΔprpDBC1/2*), Cz06 (*ΔmcmAB*, *ΔprpDBC1/2*), Cz07 (*ΔprpDBC1/2::prpE*), Cz08 (*cglp3::pcc*), Cz09 (*ΔprpDBC1/2::prpE, cglp3::pcc*), Cz10 (*ΔprpDBC1/2::aspA*, *cglp3::panD*). All data represent the mean ± SD, and error bars indicate the standard error (n = 3).

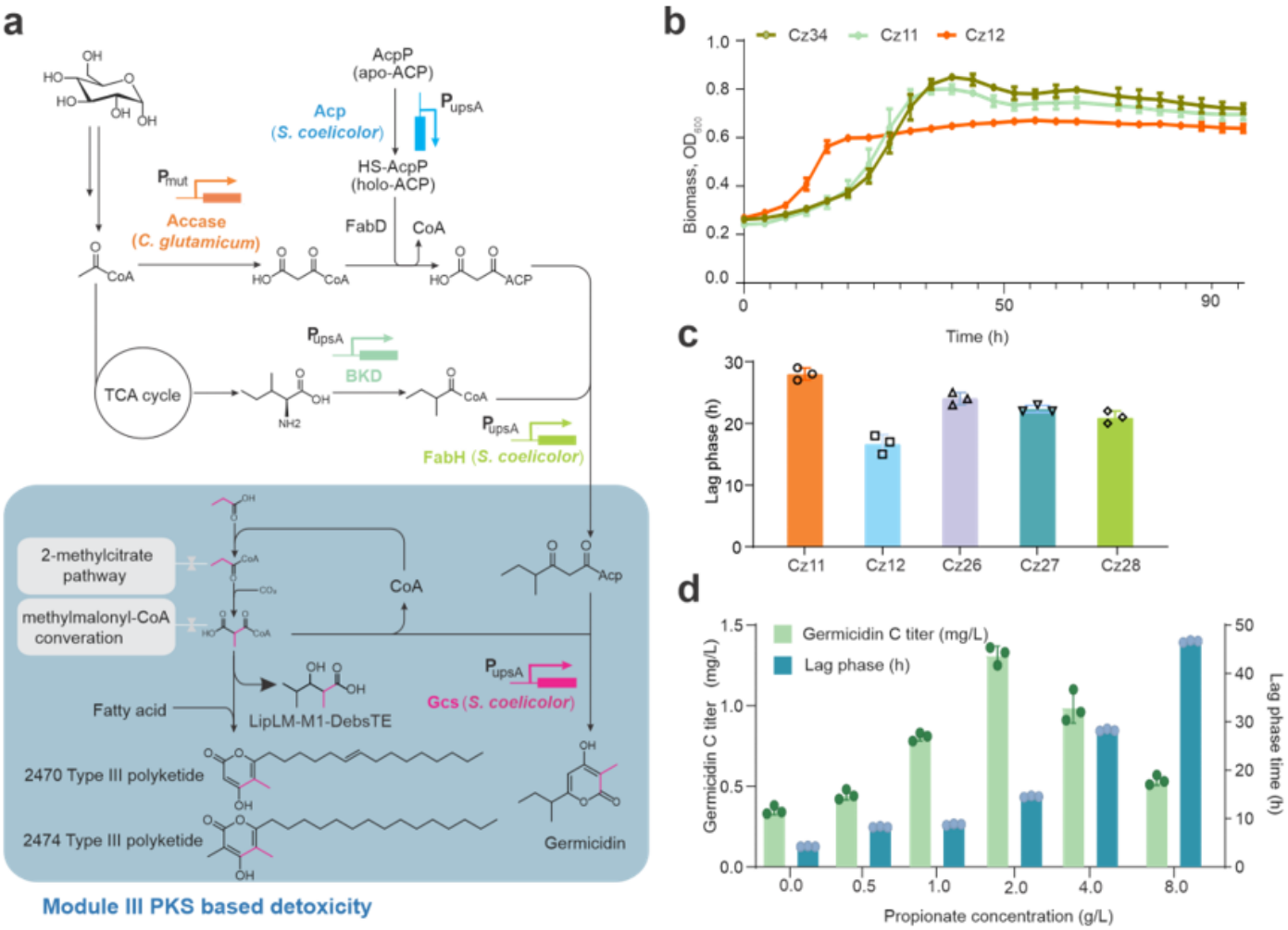

Figure 4

Methylmalonyl-CoA–dependent germicidin and 3-hydroxyacid production can rescue cell growth in propionate-containing medium. a: Pathways involved in production of germicidin and 3-hydroxyacids from glucose and propionate. Illustrated by each reaction is the name of the enzyme, the name of the organism from which it was derived, and the identity of the promoter used to drive its expression. The pink lines in the chemical structures of propionate, propionyl-CoA, methylmalonyl-CoA, and germidicin indicate the labeled carbons when cells were cultivated in [^{13}C]propionate. b: Growth curves of different strains in CGXII minimal medium with 0.6 g/L propionate. Cz34 (*ΔmcmAB*, *ΔprpDBC1*, *prpDBC2*::*sfp*), Cz11 (Cz34 *cglp3*::*rfp*), Cz12 (entire germicidin pathway genes integrated into Cz34) c: Lag phase comparison of strains containing various PKSs in CGXII minimal medium with 0.6 g/L propionate. Cz26 (LipLM-M1-debsM6TE integrated into Cz34), Cz27 (Type III PKS 2470 integrated into Cz34), Cz28 (Type III PKS 2474 integrated into Cz34). d: Germicidin C titer and lag phase in Cz12 cultivated in different concentrations of propionate. All data represent the mean ± SD, and error bars indicate the standard error (n = 3).

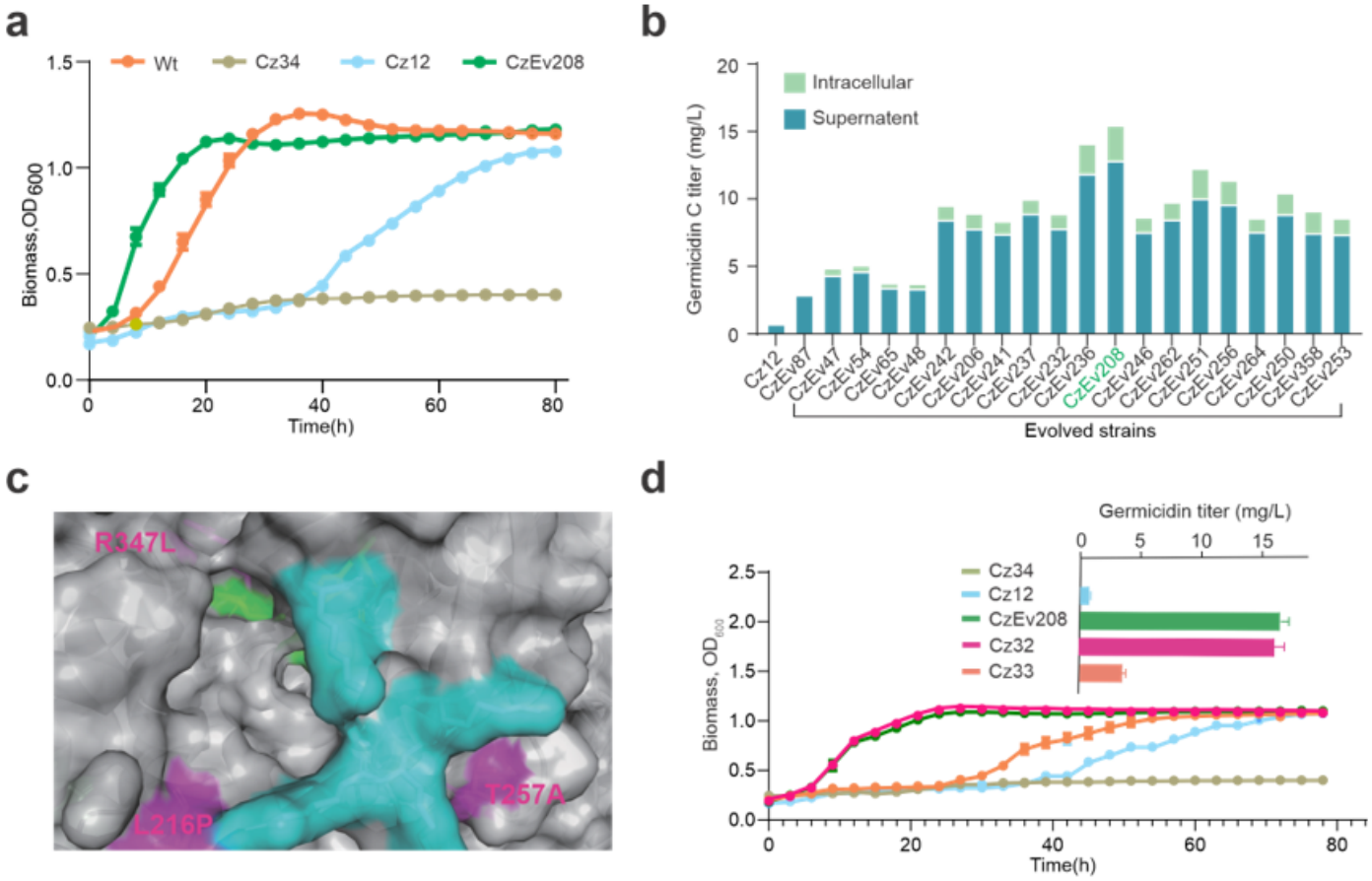

Figure 5

Evolved germicidin production strains show increased titer and improved growth. a: Growth curves of Cz34 (no germicidin pathway), Cz12 (germicidin pathway integrated into Cz34), and CzEv208 (single colony from evolved population of Cz13) in CGXII minimal medium with 8 g/L propionate. For comparison, we included the growth curve of WT in CGXII minimal medium without propionate. b: Comparison of germicidin production among Cz12 and 20 evolved strains. c: Modeled surface structure of Gcs based on PDB structure 3v7i.1.A[39]. Residues that were mutated in evolved strains are labeled. Pink represents mutation sites L216P, T257A and R347L. Active site catalytic triad residues Cys175-His312-Asn346 are shown in green. Cyan represents four Arg (276/277/280/317) residues adjacent to the catalytic triad active site[39]. d: Growth of and germicidin titers produced by various reverse engineered strains. Inset shows germicidin C titer for each strain. Cz13 (evolved strains, which is a population containing lots of different mutation strains), Cz32 (evolved *gcs* in CzEv208 replaced with native *gcs*), Cz33 (native *gcs* in Cz12 replaced with Gcs R347L). All data represent the mean ± SD, and error bars indicate the standard error (n = 3).

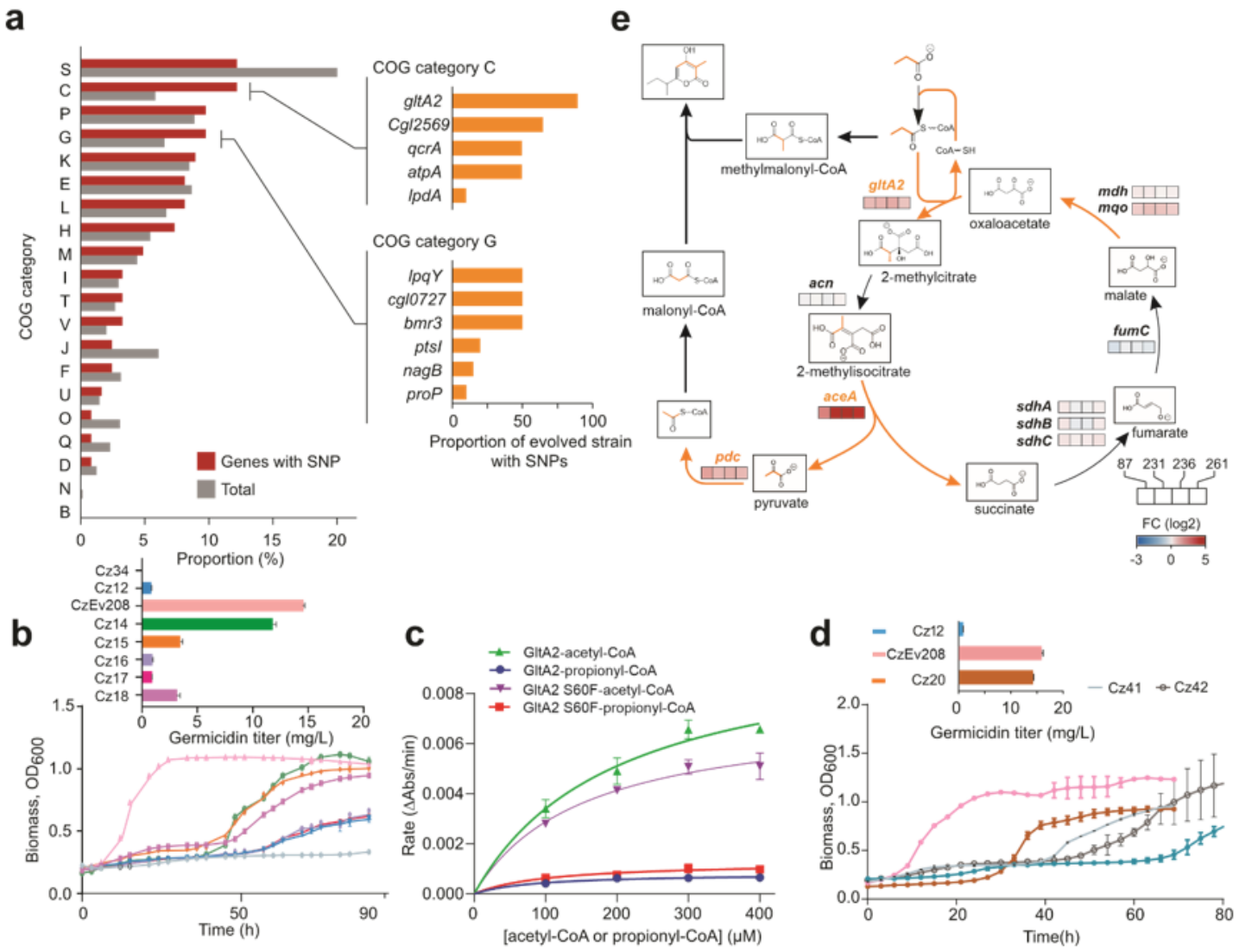

Figure 6

Propionyl-CoA conversion to germicidin by GltA2-based methylcitrate pathway. a: Clusters of orthologous groups (COG) analysis of SNPs using EggNOG[43]. Left panel: distribution of total genes and SNP-containing genes in various COG categories. Right panel: proportion of 19 evolved strains having SNPs in the corresponding genes assigned to COG categories C and G. b: Growth curves of (bottom) and germicidin titers produced by (top) strains with specific *gltA* mutations in CGXII minimal medium with 8 g/L propionate. c: *In vitro* citrate synthase assay using purified GltA2 proteins. Acetyl-CoA and/or propionyl-CoA are consumed in the reaction, releasing free CoA-SH which is measured colorimetrically. d: Growth curves of (bottom) and germicidin titers produced by (top) various *gltA2* based strains. e: GltA2-based methylcitrate pathway. The orange bond in each molecule represents [^{13}C]labeled carbon. All data represent the mean ± SD, and error bars indicate the standard error (n = 3).

Supplementary Files

This is a list of supplementary files associated with this preprint. Click to download.

- SupplementaryInformationjdk.docx